



Molecular mechanisms of DNase inhibition of early biofilm formation *Pseudomonas aeruginosa* or *Staphylococcus aureus*: A transcriptome analysis

Wusheng Deng^{a,b,1}, Chuanlin Zhou^{a,1}, Jiaoxia Qin^{a,1}, Yun Jiang^{a,c}, Dingbin Li^d, Xiuji Tang^a, Jing Luo^a, Jinliang Kong^{a,*}, Ke Wang^{a,**}

^a Department of Respiratory and Critical Care Medicine, The First Affiliated Hospital of Guangxi Medical University, Nanning, Guangxi, China

^b Department of Respiratory and Critical Care Medicine, Hunan Provincial People's Hospital/The First Affiliated Hospital of Hunan Normal University, Changsha, Hunan, China

^c Department of Respiratory and Critical Care Medicine, The First Affiliated Hospital of Shaoyang University, Shaoyang, Hunan, China

^d Department of Orthopedic Trauma and Hand Surgery, The First Affiliated Hospital of Guangxi Medical University, Nanning, Guangxi, China

ARTICLE INFO

Keywords:

DNase
Pseudomonas aeruginosa
Staphylococcus aureus
Transcriptome analysis
Biofilm

ABSTRACT

In vitro studies show that DNase can inhibit *Pseudomonas aeruginosa* and *Staphylococcus aureus* biofilm formation. However, the underlying molecular mechanisms remain poorly understood. This study used an RNA-sequencing transcriptomic approach to investigate the mechanism by which DNase I inhibits early *P. aeruginosa* and *S. aureus* biofilm formation on a transcriptional level, respectively. A total of 1171 differentially expressed genes (DEGs) in *P. aeruginosa* and 1016 DEGs in *S. aureus* enriched in a variety of biological processes and pathways were identified, respectively. Gene Ontology (GO) and Kyoto Encyclopedia of Genes and Genomes (KEGG) enrichment analyses revealed that the DEGs were primarily involved in *P. aeruginosa* two-component system, biofilm formation, and flagellar assembly and in *S. aureus* biosynthesis of secondary metabolites, microbial metabolism in diverse environments, and biosynthesis of amino acids, respectively. The transcriptional data were validated using quantitative real-time polymerase chain reaction (RT-qPCR), and the expression profiles of 22 major genes remained consistent. These findings suggested that DNase I may inhibit early biofilm formation by downregulating the expression of *P. aeruginosa* genes associated with flagellar assembly and the type VI secretion system, and by downregulating *S. aureus* capsular polysaccharide and amino acids metabolism gene expression, respectively. This study offers insights into the mechanisms of DNase treatment-based inhibition of early *P. aeruginosa* and *S. aureus* biofilm formation.

1. Introduction

Biofilm-related infections, which account for 65–80% of all infections, can cause serious health problems [1]. Despite recent advancements in the treatment of biofilm-related infections, these infections remain associated with high morbidity and mortality rates [2, 3]. An increase in antibiotic resistance threatens treatment efficacy. Antibiofilm therapies can successfully impede antibiotic resistance and thus provide new treatment option for biofilm-related infections.

Biofilms are sessile communities of microbes surrounded by a self-produced polymer matrix [4,5]. *Pseudomonas aeruginosa* (*P. aeruginosa*) and *Staphylococcus aureus* (*S. aureus*) are responsible for a significant

number of biofilm-related infections [6,7]. Biofilm-related microbial cells are less susceptible to antimicrobials and more resistant to be attacked by host immune effector mechanisms [8]. Microbial cells within biofilms are 10–1000 times more resistant to antibiotics than free-living bacteria cells [9]. In biofilm-related infections, microbial cells establish antibiotic-resistant biofilms, which are recalcitrant to clearance and are associated with serious adverse medical outcomes [10]. Inhibiting biofilm formation is a viable approach to improve the efficacy of antimicrobials.

DNase degrades extracellular DNA present in the matrix of biofilms and can inhibit or disperse *P. aeruginosa* and *S. aureus* biofilms [11,12]. DNase can also increase antibiotic susceptibility, and in combination of antibiotics, improve the function of antibiofilm against biofilm-

* Corresponding author.

** Corresponding author.

E-mail addresses: kjl071@163.com (J. Kong), keewang@hotmail.com (K. Wang).

¹ These authors have contributed equally to this work and share first authorship.

associated pathogens [13]. While DNase is effective against early biofilms, however, this enzyme has no apparent effect on mature biofilms [14]. Meanwhile the underlying molecular mechanism for the effect of DNase against early biofilms remains poorly understood.

RNA-sequencing (RNA-seq) is a powerful technique that is widely used to evaluate bacterial antibiofilm mechanism on the transcriptional level [15]. This method has the advantage of detecting the overall transcription of any species at the single nucleotide level. RNA-seq allows the quantitative analysis of gene expression and a better understanding of biological processes [16]. Thus, this method is ideal for investigating the underlying molecular mechanism of anti-biofilm agents.

Our previous study [17] demonstrated that DNase I inhibited early (24 h) biofilm formation in *P. aeruginosa* and *S. aureus* both *in vitro* and *in vivo*. The current study sought to further investigate global transcriptional changes using RNA-seq analysis to better understand the mechanism of DNase on early (24 h) *P. aeruginosa* and *S. aureus in vitro* biofilm formation.

2. Methods

2.1. Chemicals, bacteria, and culture media

DNase I (Baoriyi Biotechnology Beijing, China), with an activity of 5 U/L, was derived from a non-animal host and stored at -20°C . The *P. aeruginosa* PAO1 wild-type strain and *S. aureus* ATCC25913 standard strain were used for the current study. Both strains were stored in Luria-Bertani (LB) broth containing 25% glycerol at -80°C . The PAO1 strains were grown in LB, and *S. aureus* standard strains were grown in tryptic soy broth supplemented with 0.5% glucose. The bacterial suspension was diluted to an absorbance at OD600 of 0.1, and then serially diluted to 10^6 CFU/mL.

2.2. Sample treatment and collection

The bacterial suspension was transferred to a 24-well titer plate. In the DNase I treated-group, DNase I was added to each plate at a final concentration of 66.7 U/mL and further cultured for 24 h. This concentration was shown to inhibit *P. aeruginosa* and *S. aureus* biofilm formation in our previous study [17]. In the control group, an equal volume of phosphate-buffered saline (PBS) was added instead of DNase I. After a 24-h culture, planktonic bacteria were gently washed with PBS, and the biofilm bacterial culture was centrifuged at 8000 g for 5 min prior to RNA extraction. In each group, triplicate samples were prepared under the same experimental conditions.

2.3. RNA extraction

The previously described RNA extraction method was used with minor modifications (Zheng et al., 2018). In brief, total RNA was extracted using RNAiso Plus (Takara Holdings, Kyoto, Japan). The *S. aureus* suspension was suspended in a 100- μL mixture of lysostaphin (recombinant; 1 mg/mL; Sangon) and lysozyme (25 mg/mL; Sangon), and incubated at 37°C for 1 h before extraction. The PAO1 suspension was suspended in lysozyme (0.4 mg/mL), and incubated at 37°C for 20 min. Chloroform was then added to the lysate and the supernatant was transferred to an enzyme-free tube with isopropanol. The RNA was precipitated with 75% cold ethanol and collected by centrifugation. RNA integrity was assessed using the RNA Nano 6000 Assay Kit from the Bioanalyzer 2100 system (Agilent Technologies, CA, USA).

The RNA from each sample was used for transcriptome sequencing and quantitative real-time polymerase chain reaction (RT-qPCR).

2.4. Library construction

mRNA was purified from total RNA using probes from the Ribo-Zero

Plus rRNA Depletion Kit (illumina/20037135) to remove rRNA. Fragmentation was performed using divalent cations in First Strand Synthesis Reaction Buffer ($5\times$). First-strand cDNA was synthesized using random hexamer primer and M-MuLV Reverse Transcriptase and RNaseH treatment was used to degrade the RNA. In the DNA polymerase I system, dUTP was used to replace the dNTP of dTTP as the raw material to synthesize the second strand of cDNA. The remaining overhangs were converted into blunt ends using exonuclease/polymerase. After the adenylation of 3' ends of the DNA fragments, adaptors with a hairpin loop structure were ligated to prepare for hybridization. USER Enzyme was used to degrade the second strand of cDNA containing U. To select cDNA fragments of preferentially 370–420 bp in length, the library fragments were purified using the AMPure XP system (Beckman Coulter, Beverly, USA). PCR was then performed using Phusion High-Fidelity DNA polymerase, universal PCR primers, and the Index (X) Primer. The PCR products were purified (AMPure XP system) and library quality was assessed using the Agilent 2100 Bioanalyzer system.

2.5. Transcriptome sequencing

Clustering of the index-coded samples was performed on a cBot Cluster Generation System using TruSeq PE Cluster Kit v3-cBot-HS (illumina) according to the manufacturer's instructions. After cluster generation, the library preparations were sequenced on an illumina NovaSeq platform and 150 bp paired-end reads were generated.

2.6. Quality control

Raw data (raw reads) in the fastq format was initially processed using fastp software. In this step, clean data (clean reads) were obtained by removing reads containing adapters or ploy-N and low-quality reads from the raw data. At the same time, the Q20, Q30, and GC content of the clean data were calculated. All further analyses were conducted using clean and high-quality data.

2.7. Reads mapping to the reference genome

Reference genome and gene model annotation files were downloaded directly from the genome website. Building the index and aligning the clean reads to the reference genome were conducted using Bowtie 2-2.2.3.

2.8. Quantification of gene expression

FeatureCounts v1.5.0-p3 was used to count the reads mapped to each gene. The fragments per kilobase of transcript sequence per million mapped fragments (FPKM) of each gene were then calculated according to its length and read count. This is the most common method used to estimate gene expression because it simultaneously considers the effect of sequencing depth and gene length on read count.

2.9. Analysis of differentially expression genes (DEGs)

Differential expression analysis of two groups (control group and DNase I-treated group) was performed using the DESeq R package (1.18.0). DESeq provides statistical routines for determining the differential expression of digital gene expression data using a model based on the negative binomial distribution. The resulting P-values were adjusted using the Benjamini and Hochberg approach for controlling the false discovery rate. Genes with an adjusted P-value of <0.05 found by DESeq were assigned as differentially expressed.

2.10. GO and KEGG enrichment analysis

Gene Ontology (GO) enrichment analysis of DEGs was implemented using the Goseq R package, in which gene length bias was corrected. GO

Table 1Summary of RNA-seq data from *P. aeruginosa* or *S. aureus* treated with DNase I.

Sample name	Raw reads	Clean reads	Raw bases	Clean bases	Q20 (%)	Q30 (%)	Total mapping rate
<i>P. aeruginosa</i>							
CP1	15,945,828	15,820,540	2.4G	2.4G	98.39	95.33	93.83%
CP2	17,583,572	17,386,224	2.6G	2.6G	98.41	95.35	94.49%
CP3	15,401,600	15,244,658	2.3G	2.3G	98.51	95.59	95.57%
DP1	15,075,116	14,937,782	2.3G	2.2G	98.59	95.71	93.88%
DP2	15,671,964	15,519,966	2.4G	2.3G	98.5	95.5	93.99%
DP3	15,216,034	14,971,616	2.3G	2.2G	98.46	95.34	95.03%
<i>S. aureus</i>							
CS1	14,989,000	14,793,238	2.2G	2.2G	98.4	94.68	95.07%
CS2	15,241,410	15,007,782	2.3G	2.3G	98.26	94.33	94.85%
CS3	16,573,598	16,226,984	2.5G	2.4G	98.4	94.74	95.04%
DS1	15,409,208	15,210,890	2.3G	2.3G	98.3	94.45	93.89%
DS2	15,284,242	15,119,798	2.3G	2.3G	98.43	94.7	93.98%
DS3	15,847,888	15,603,368	2.4G	2.3G	98.35	94.62	90.60%

CP, control *P. aeruginosa* group; DP, DNase I-treated *P. aeruginosa* group; CS, control *S. aureus* group; DS, DNase I-treated *S. aureus* group.

terms with a corrected P value < 0.05 were considered significantly enriched by DEGs. Kyoto Encyclopedia of Genes and Genomes (KEGG) is a database resource for understanding high-level functions and utilities of the biological system, including the cell, the organism and the ecosystem, using molecular-level information often obtained from large-scale molecular datasets generated by genome sequencing and other high-throughput experimental technologies (<http://www.genome.jp/kegg/>). KOBAS software was used to test the statistical enrichment of DEGs in the KEGG pathways.

2.11. RT-qPCR

Expression in *P. aeruginosa* genes (*tssC*, *tssB*, *tse 3*, *pchC*, *pchG*, *pchF*, *feoA*, *fptA*, *flgK*, *fliN*, and *pscQ*) and *S. aureus* genes (*hla*, *SAOUHSC_00812*, *SAOUHSC_00008*, *SAOUHSC_01787*, *SAOUHSC_00569*, *Cap8F*, *Cap5D*, *Cap8C*, *Cap5B*, *sar A*, *agr A*) was evaluated by RT-qPCR at the mRNA level. RNA (1 µg) was used for cDNA synthesis using the PrimeScript second-strand cDNA synthesis kit (cat. RR047A, Takara). RT-qPCR was performed with SYBR Green II (cat. RR047A, Takara) using a LightCycler 480 II real-time PCR system (Roche) with the specific primers listed in [Supplementary Table S1](#). The data were calculated using the $2^{-\Delta\Delta Ct}$ method

according to a previous study [18].

2.12. Staining of crystal violet stain in biofilms

The overnight cultures were inoculated in the absence or presence of DNase I (final concentration = 66.7 U/mL) onto 13 × 13 mm glass slides in a 24-well titer plate. After 24 h of incubation at 37 °C, we gently washed the glass slides and stained them with a 0.1% crystal violet ammonium oxalate solution (100 mL; Beijing Solarbio Science & Technology Co., Ltd., Beijing, China) for 20 min. After washing with PBS and careful drying, we visualized and photographed the samples under a fluorescence microscope (Nikon eclipse Ni, Tokyo, Japan).

3. Results

3.1. Transcriptome sequencing and clustering DEGs

Raw reads data were sequenced and filtered for further analysis, yielding approximately 14.97–17.39 million clean reads for *P. aeruginosa*, and 14.98–16.57 million clean reads for *S. aureus*. The number of high-quality clean reads in both the DNase I-treated group

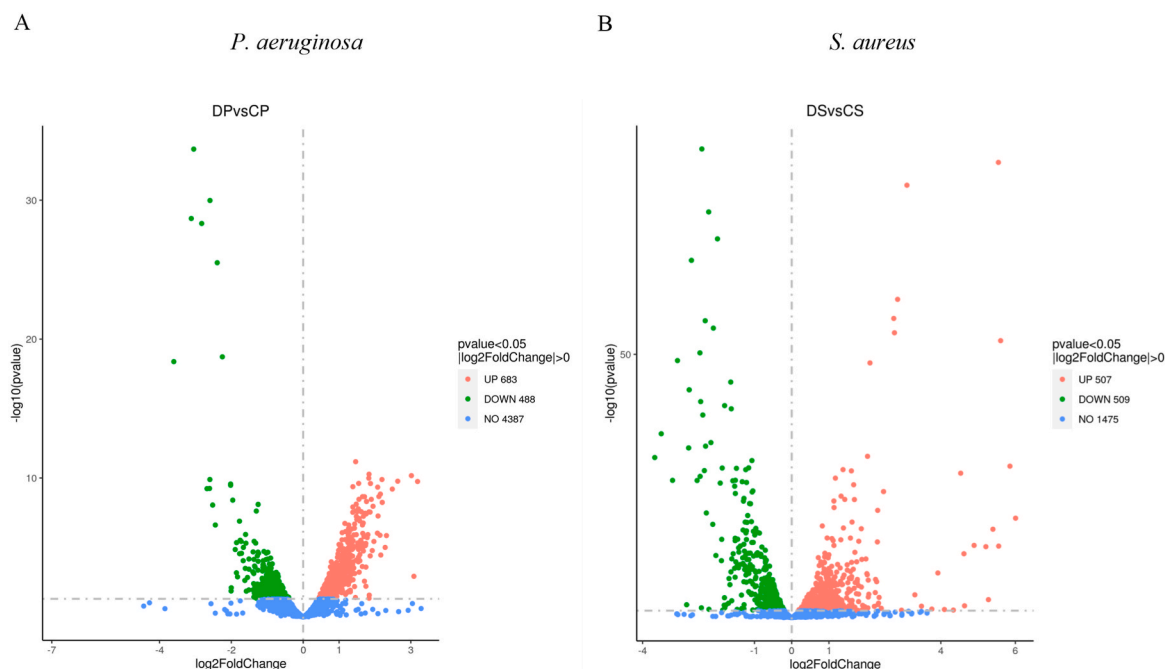


Fig. 1. Volcano graph of DEGs and up-regulated and down-regulated genes in *P. aeruginosa* and *S. aureus*, between the DNase I-treated group and control group.

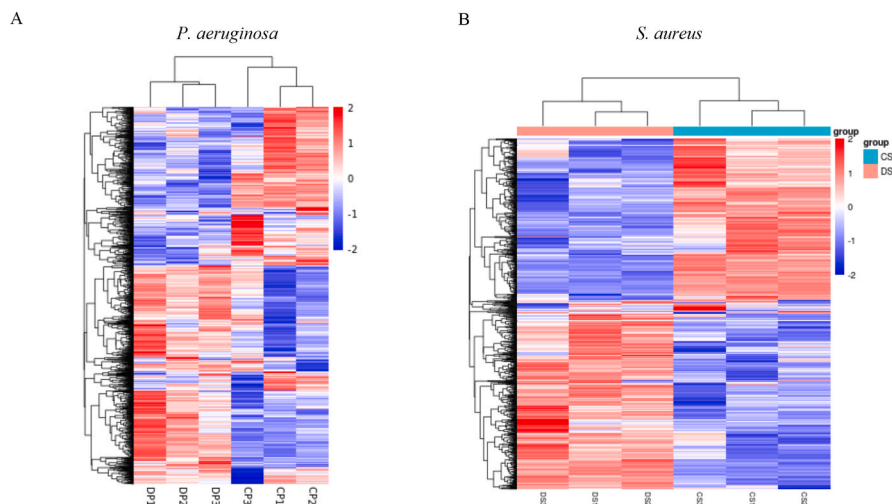


Fig. 2. Heatmap expression pattern clustering analysis of the DNase I-treated group and control group.

Table 2

The top 20 DEGs of *P. aeruginosa* genes between DNase I-treated group and control group.

GeneName	log2FoldChange	P value	up-regulated or down-regulated
<i>pchB</i>	3.603	4.18E-19	down-regulated
<i>pchA</i>	3.115	2.10E-29	down-regulated
<i>fptA</i>	3.048	2.12E-34	down-regulated
<i>kdpA</i>	3.087	0.001187	up-regulated
<i>lecA</i>	3.016	6.79E-11	up-regulated
<i>pchD</i>	2.825	4.78E-29	down-regulated
<i>pmrA</i>	2.606	5.70E-10	down-regulated
<i>speD</i>	2.598	1.29E-10	down-regulated
<i>pchE</i>	2.594	1.06E-30	down-regulated
<i>pmrB</i>	2.445	2.40E-07	down-regulated
<i>pchF</i>	2.392	3.21E-26	down-regulated
<i>kdpB</i>	2.284	9.87E-06	up-regulated
<i>hslV</i>	2.087	5.38E-08	up-regulated
<i>pchG</i>	2.005	0.0135	down-regulated
<i>pumA</i>	1.946	1.07E-08	up-regulated
<i>mexG</i>	1.865	2.83E-08	up-regulated
<i>vgrG</i>	1.857	0.00066	down-regulated
<i>leuB</i>	1.854	4.46E-06	down-regulated
<i>grpE</i>	1.785	1.94E-06	up-regulated
<i>cprA</i>	1.771	1.27E-07	down-regulated

and control group was >98.39% for *P. aeruginosa*, and 98.26% for *S. aureus*. The rate of low-quality reads was <0.02% (Table 1). These results suggested good quality that the sequencing data were of good quality.

The high-quality clean reads were aligned with the rRNA and mapped to the reference genome. Transcriptome sequencing data were deposited into the NCBI SRA database (SRA accession: PRJNA916182). Using an FDR threshold ≤ 0.05 and a $|\log_2 \text{fold change (FC)}| > 0$ in the *P. aeruginosa* group, 1171 significant DEGs were identified, of which 683 were up-regulated and the remaining 488 genes were down-regulated in the DNase I-treated group vs. control group; In the *S. aureus* group, 1016 significant DEGs were identified, of which 507 genes were up-regulated and the remaining 509 genes were down-regulated in the DNase I-treated group vs. control group (Fig. 1). The heat map shown in Fig. 2 shows those genes with the most significant alterations in transcript levels in the DNase I-treated group as compared to the control group. The top 20 DEGs *P. aeruginosa* DEGs in the DNase I-treated group were identified as: *pchB*, *pchA*, *fptA*, *kdpA*, *lecA*, *pchD*, *pmrA*, *speD*, *pchE*, *pmrB*, *pchF*, *kdpB*, *hslV*, *pchG*, *pumA*, *mexG*, *vgrG*, *leuB*, *grpE*, and *cprA* (Table 2) and the top 20 in *S. aureus* DEGs in the DNase I-treated group were identified as: SAOUHSC_02451, SAOUHSC_02450, SAOUHSC_00914, SAOUHSC_02452, SAOUHSC_02449,

Table 3

The top 20 DEGs of *S. aureus* genes between DNase I-treated group and control group.

GeneName	log2FoldChange	P value	up-regulated or down-regulated
SAOUHSC_02451	6.006	1.31E-19	up-regulated
SAOUHSC_02450	5.855	1.81E-29	up-regulated
SAOUHSC_00914	5.605	2.54E-53	up-regulated
SAOUHSC_02452	5.552	2.68E-14	up-regulated
SAOUHSC_02449	5.545	3.54E-87	up-regulated
SAOUHSC_00915	5.398	1.65E-17	up-regulated
SAOUHSC_02432	5.278	0.0004	up-regulated
SAOUHSC_02453	5.209	3.43E-14	up-regulated
SAOUHSC_02454	4.892	1.97E-14	up-regulated
SAOUHSC_02657	4.636	0.0059	up-regulated
SAOUHSC_02455	4.620	7.60E-13	up-regulated
SAOUHSC_00916	4.532	3.93E-28	up-regulated
SAOUHSC_02717	4.336	0.0385	up-regulated
SAOUHSC_T00049	4.096	0.0298	up-regulated
SAOUHSC_T0006	3.920	3.43E-09	up-regulated
SAOUHSC_00289	3.758	0.0248	up-regulated
SAOUHSC_00115	3.674	4.08E-31	down-regulated
SAOUHSC_00116	3.499	1.24E-35	down-regulated
SAOUHSC_03042	3.480	0.0071	up-regulated
SAOUHSC_00243	3.302	4.85E-05	up-regulated

SAOUHSC_00915, SAOUHSC_02432, SAOUHSC_02453, SAOUHSC_02454, SAOUHSC_02657, SAOUHSC_02455, SAOUHSC_00916, SAOUHSC_02717, SAOUHSC_T00049, SAOUHSC_T0006, SAOUHSC_00289, SAOUHSC_00115, SAOUHSC_00116, SAOUHSC_03042, and SAOUHSC_00243 (Table 3).

3.2. Functional annotation and pathway analysis of DEGs

GO analysis provides a set of dynamic, controlled, and structured

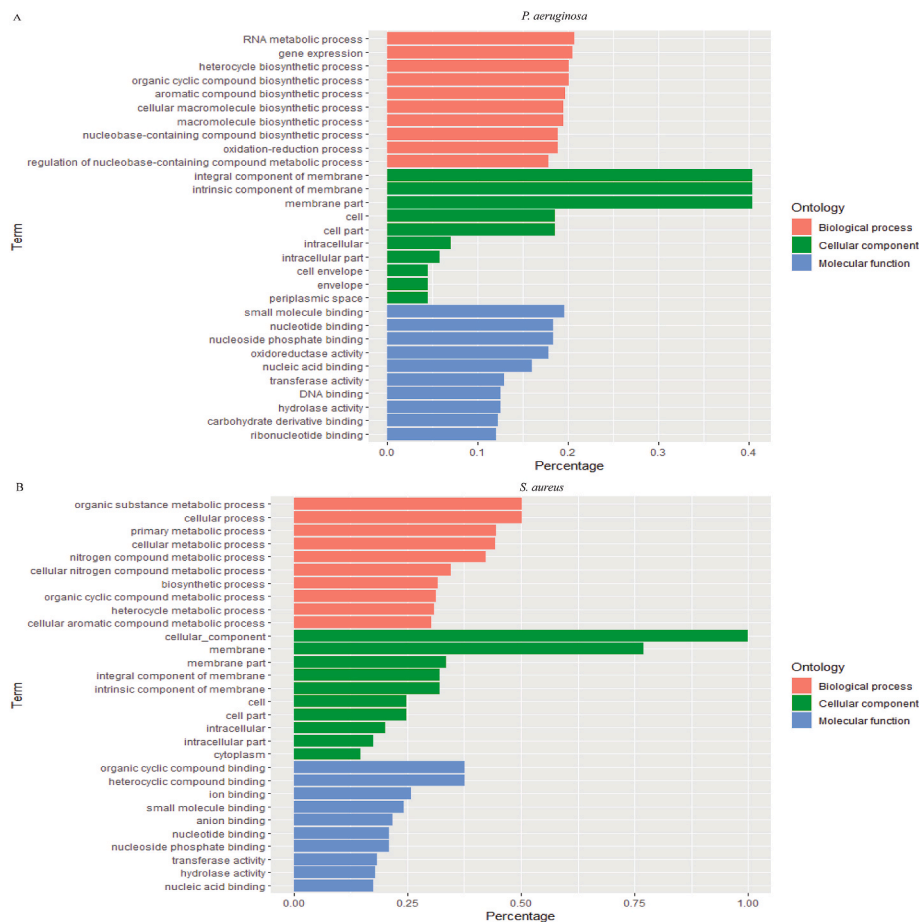


Fig. 3. Functional comparison of DEGs in the DNase I treated-group compared to the control group. Functions are organized into three groups, namely Cellular components, Molecular Function, and Biological Process.

terminologies to describe gene functions and products in an organism. According to GO functions, all DEGs are classified into three categories as: biological process (BP), cellular component (CC), and molecular function (MF) (Fig. 3). The BP-related *P. aeruginosa* DEGs were mainly involved in RNA metabolic process, gene expression, and heterocycle biosynthetic process, the CC-related *P. aeruginosa* DEGs were mainly involved in integral component of membrane, intrinsic component of membrane, and the MF-related *P. aeruginosa* DEGs were mainly involved in small molecule binding and nucleotide binding. Meanwhile, the BP-related *S. aureus* DEGs were mainly involved in organic substance metabolic process, cellular process, and primary metabolic process, the CC-related *S. aureus* DEGs were mainly involved in the cellular-component, membrane and cellular component, and the MF-related *S. aureus* DEGs were mainly involved in the organic cyclic compound binding and the heterocyclic compound binding.

3.3. KEGG pathway analysis

The DEGs were also enriched in the KEGG pathways, which provide information on biological systems and their relationships at the molecular, cellular, and organism levels. The KEGG pathways were annotated from the assembled *P. aeruginosa* genes and *S. aureus* transcriptome, and the results were mapped with GO terms. Of the top 20 *P. aeruginosa* pathways involved in pathway enrichment, 40 DEGs were involved in biofilm formation, and 30 DEGs were involved in flagellar assembly (Fig. 4). Bacterial chemotaxis and propanoate metabolism were the most significantly enriched pathways ($p < 0.05$). Of these, genes involved in the *P. aeruginosa* two-component system, biofilm formation-*Pseudomonas aeruginosa*, flagellar assembly and quorum sensing signaling were

most abundant. Of the top 20 *S. aureus* pathways involved in pathway enrichment, 40 DEGs were involved in microbial metabolism in diverse environments, and 30 were involved in biosynthesis of amino acids. The citrate cycle (TCA cycle), butanoate metabolism, and 2-oxocarboxylic acid metabolism were the most significantly enriched pathways ($p < 0.05$). Genes involved in biosynthesis of secondary metabolites, microbial metabolism in diverse environments, biosynthesis of amino acids and carbon metabolism signaling were the most abundant.

3.4. Gene expression profile analysis

To validate our transcriptional analysis results, *P. aeruginosa* and *S. aureus* were treated with DNase I, and 22 genes were selected and confirmed by RT-qPCR. The candidate genes were chosen from a representative set of genes involved in regulation and signal transduction, production of the extracellular matrix and virulence factors, flagella, and iron acquisition. DNase I significantly repressed transcription levels of the selected genes (Fig. 5; $p < 0.05$).

3.5. Staining of crystal violet stain

To detect the effect of DNase I on the biofilm formation, *P. aeruginosa* or *S. aureus* biofilms were stained with crystal violet stain. From the fluorescent micrograph results, the DNase I-treated group had less biofilms accumulation than the control group (Fig. 6).

4. Discussion

Biofilm-related infections have debilitating health outcomes. Even

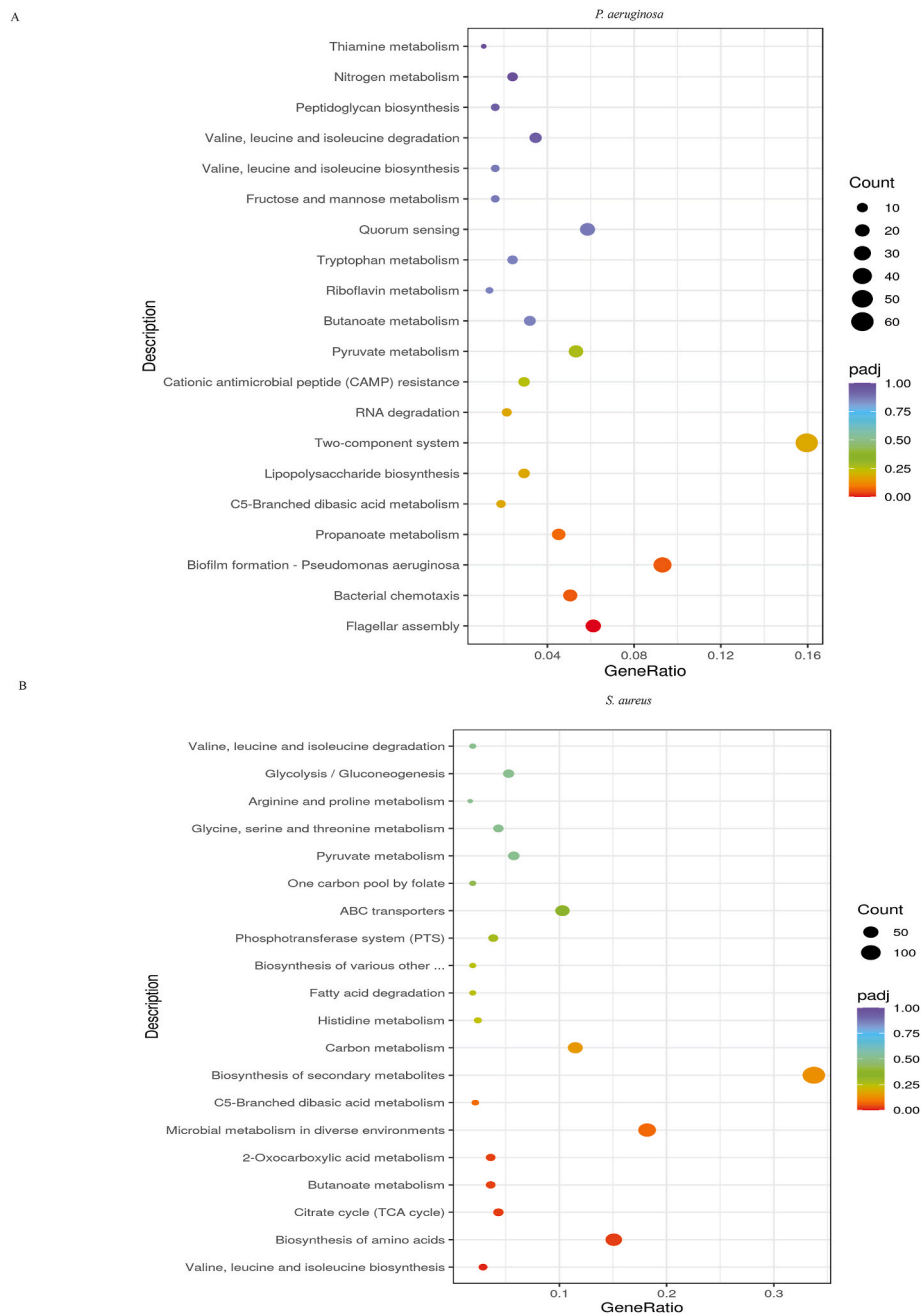


Fig. 4. KEGG enrichment of all DEGs.

after receiving appropriate antibiotic treatment, patients with biofilm-related infections have a high risk of mortality [19]. While DNase offers an antibiofilm strategy to treat biofilm-related disease, its underlying mechanism remains poorly understood [11]. Our previous study showed [17] DNase I inhibits *P. aeruginosa* and *S. aureus* early biofilm formation both *in vitro* and *in vivo*. The current study used RNA-seq transcriptome analysis to assess the underlying mechanism by which DNase I inhibits *P. aeruginosa* and *S. aureus* early biofilm formation *in vitro*. The findings suggest that DNase I may inhibit biofilm formation by downregulating the expression of genes involved in *P. aeruginosa* flagellar assembly and type VI secretion system, and downregulating the expression of *S. aureus* gene expression of capsular polysaccharide genes and amino acids metabolism.

RNA-seq has been used to investigate molecular mechanisms underlying the inhibition of biofilm formation. This technique can provide a quantitative analysis of genes expression and a better understanding of

biological processes. Qin et al. [20] used RNA-seq show that ursolic acid and resveratrol inhibit *S. aureus* biofilm formation by reducing amino acids metabolism, quorum sensing, and adhesin expression. These findings suggested that ursolic acid and resveratrol can be used to treat *S. aureus* biofilm-involved infections. Wu et al. [21] used RNA-seq to assess whether exopolysaccharide EPS273 genes were involved in biofilm formation by downregulating the *P. aeruginosa* two-component system PhoP-PhoQ and quorum sensing systems. RNA-seq provides an accurate measurement of transcript levels and their isoforms [22], providing a better understanding of the mechanistic basis of pharmaceuticals. Our RNA-seq transcriptomic analysis found that DNase I may inhibit biofilm formation by downregulating genes involved in flagellar assembly, type VI secretion system, capsular polysaccharides, and metabolism of acid metabolism. The transcriptomic results were validated using RT-qPCR.

The transcriptome sequencing results showed that the total number

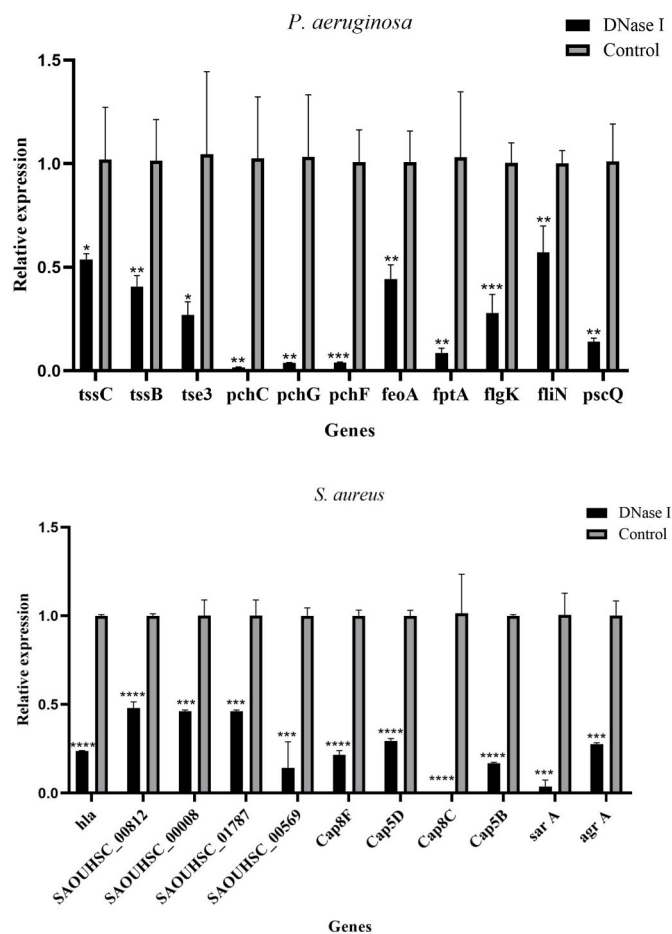


Fig. 5. Relative expression levels of selected genes in *P. aeruginosa* and *S. aureus* in the presence or absence of DNase I, as determined using real-time polymerase chain reaction. The data represent the mean \pm SD expressions. Asterisk indicates a significant difference, *indicates $p < 0.05$, **indicates $p < 0.01$, ***indicates $p < 0.001$, and ****indicates $p < 0.0001$, compared with the expression values in the control group based on t-tests ($n = 3$).

of reads and high-quality ratio reads were high and the error rate was low, indicating that the sequencing data were of good quality. The paired Pearson's coefficients co-efficient within groups were all >0.85 (Supplementary Fig. S1), demonstrating good sample correlations. Heat maps of the induced and suppressed transcripts of the DNase I samples matched to controls in the opposite way. These results demonstrated that exposure to DNase I involved a series of gene ontologies involved in biological processes, cellular component and molecular function that consequently inhibited biofilm formation.

Biofilm formation can occur through multiple pathways. Its structure is both species-specific and dependent on environmental conditions [23]. Previous studies indicate that the second messenger molecule cyclic diguanosine monophosphate, nutritional conditions, bacterial motility, type VI secretion system, and quorum-sensing regulate biofilm formation [24–26]. The current study focused on how DNase I impacts *P. aeruginosa* and *S. aureus* DEGs involved in biofilm formation. KEGG analysis showed that the DEGs were mainly involved in the *P. aeruginosa* two-component system, biofilm formation-Pseudomonas aeruginosa, flagellar assembly and quorum sensing signaling pathway, and involved in *S. aureus* biosynthesis of secondary metabolites, microbial metabolism in diverse environments, biosynthesis of amino acids and carbon metabolism. These findings suggested that DNase I primarily inhibits biofilm formation by impacting metabolism and cell signaling.

Bacteria rely on flagella to adhere to an attachment surface, and swim to the surface of the biofilms, making it continuously thicker.

Flagellar-mediated motility is involved in the formation of *P. aeruginosa* biofilms [27]. In addition, flagellar interactions promote the formation of bacterial biofilms and maintain their structure through contact with the surfaces of adjacent colonies [28]. *P. aeruginosa* flagellar assembly pathway genes are significantly repressed after the application of an antibiofilm agent [29,30]. The most significantly enriched GO items of downregulated BP genes included those involved in flagellum-dependent cell motility and cell motility. The expression of several flagellar assembly genes including *pscL*, *flhN*, *flgH*, and *flgK*, were also significantly repressed, suggesting that DNase I likely inhibits *P. aeruginosa* biofilm formation preventing flagella assembly and bacterial movement. However, whether DNase inhibits *P. aeruginosa* flagella-mediated motility requires further validation.

Bacterial cells communicate with their surrounding environment through secretion systems. *P. aeruginosa* is associated with a type VI secretion system [31] that inhibits the growth of neighboring bacterial cells using a contact-mediated mechanism [32]. This system is also associated with *P. aeruginosa* biofilm formation and environmental adaptation [33]. Expression of type VI secretion system genes, including *hcp 1*, *hcp 2*, *hcp 3*, and *lasR*, were significantly higher in the biofilm than in *P. aeruginosa* planktonic cells. The current study found that the most significantly enriched GO items of downregulated BP genes were those involved in biofilm formation- *P. aeruginosa*. Type VI secretion system genes, which are involved in *P. aeruginosa* biofilm formation, were significantly downregulated after DNase I treatment (Supplementary Table S2), suggesting that DNase I is likely to inhibit biofilm formation by inhibiting type VI secretion system.

Capsular polysaccharides are the primary components of pathogenic microorganisms capsules, which are integral to the process of bacterial colonization and infection. In the early stage of biofilm formation, bacteria activate the expression of specific genes, promote the synthesis of extracellular polysaccharides, and downregulate the expression of capsular polysaccharides [34]. Capsular polysaccharides also hinder the adhesion of pathogenic bacteria to host cells and are inversely related to biofilm formation [35]. A prior study found that the capsular genotype and phenotype are associated with the degree of *S. aureus* biofilm formation [36]. The current study showed that the most significantly enriched GO items of downregulated BP genes were those involved in microbial metabolism in diverse environments. Capsular polysaccharides on the bacterial cell surface participate in many physiological activities, including intercellular signaling, an adhesive substance, resisting diverse adverse external environment stimulation, and biofilm formation [37–39], illustrating that their association with microbial metabolism in diverse environments. The present study found that capsular polysaccharides genes were significantly downregulated following DNase I treatment (Supplementary Table S3), suggesting that DNase I is likely to inhibit *S. aureus* biofilm formation by preventing capsular polysaccharides.

DNase cleaves DNA and provides thus the cell by nutrients (such as nitrogen and phosphorus), one could expect the activation of systems involved in nitrogen and phosphorus metabolism. DNase cleaves extracellular DNA, and the cleaved small molecules can enter cells as nitrogen and carbon sources, resulting in a series of gene expression changes. In our RNAseq data, few genes involved in nitrogen metabolism were significantly changed following DNase I treatment (Supplementary Table S4), and genes involved in phosphorus metabolism were not significantly changed following DNase I treatment, suggesting that DNase I is unlikely to inhibit biofilm formation by nitrogen and phosphorus metabolism.

A transposon insertion screen and RNA-Seq were previously used to identify genes involved in eDNA release during *S. aureus* biofilm formation [40]. These findings illustrated that impaired cell wall homeostasis reduced cyclic-di-AMP levels involved in triggering eDNA release. The current study used RNA-Seq and RT-qPCR to investigate the mechanisms and consequences underlying the *P. aeruginosa* and *S. aureus* biofilm inhibition by DNase I. *P. aeruginosa* and *S. aureus*, are

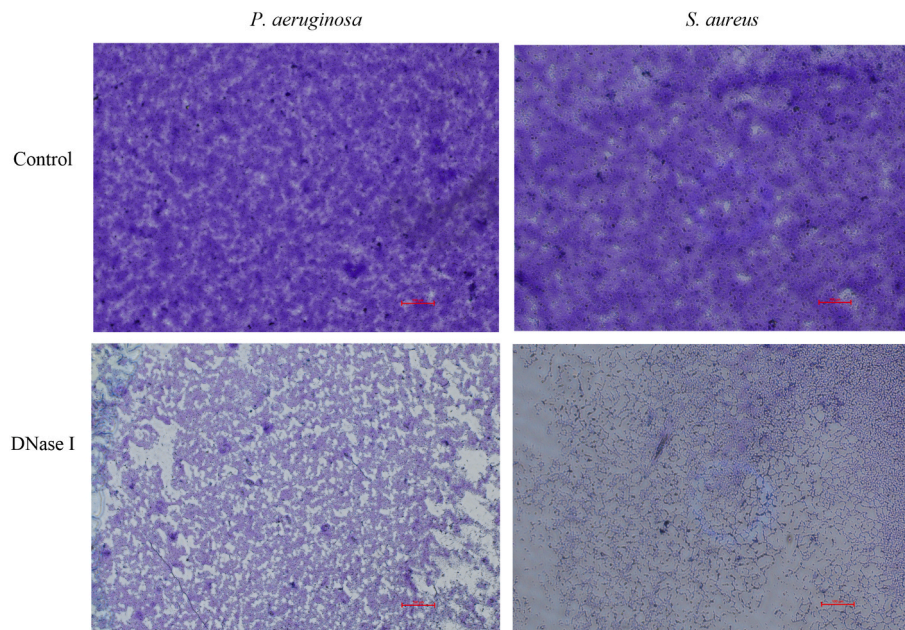


Fig. 6. Fluorescence microscopy images of *P. aeruginosa* or *S. aureus* biofilms ($100\times$). Crystal violet ammonium oxalate solution-stained biofilms in purple. In the DNase I group, the extent of crystal violet stain decreased compared with the extent in the drug-free control group.

prototype Gram-negative and Gram-positive pathogens, respectively, with the remarkable capacity to form biofilms. Investigating how the biofilms of these species are inhibited will inform methods for controlling biofilms in clinical settings.

This study has some limitations. First, the DNase I-related mechanisms of inhibiting biofilm formation were only observed in *P. aeruginosa* and *S. aureus*, and the mechanism by which DNase I eradicates biofilm was not explored. Second, RT-qPCR only identified genes that were downregulated following DNase I treatment in *P. aeruginosa* and *S. aureus*. Third, while amino acid metabolism is regulated by multiomics, including genomics, proteomics, and metabolomics, the current study explored genomics, providing that many of the functions and pathways involved in downregulating gene enrichment were related to amino acid metabolism, suggesting that DNase I may inhibit biofilm formation by inhibiting the amino acid metabolism of *S. aureus*, but did not explore metabolomics. The role of DNase I metabolomics on the inhibition of biofilm formation will require additional study.

In conclusion, the transcriptome analysis performed in this study suggested that DNase I has different mechanisms for inhibiting *P. aeruginosa* and *S. aureus* biofilm formation. This may occur by downregulating the expression of genes involved in *P. aeruginosa* flagellar assembly and the type VI secretion system, and by downregulating *S. aureus* capsular polysaccharides and amino acids metabolism gene expression, respectively. The findings offer insights into the mechanisms of DNase treatment-based inhibition of early *P. aeruginosa* and *S. aureus* biofilm formation.

Funding

This work was supported by National Natural Science Foundation of China (No. 82260023, 82104499, 82160783, and 81760743); the Natural Science Foundation of Guangxi Province (No. 2022GXNSFAA035646); the Key Research Program of Guangxi Science and Technology Department (No. AB21196010); the Health and Family Planning Commission of Guangxi Zhuang Autonomous Region, self-funded projects (No. Z20200825); Guangxi Health Commission Key Lab of Fungi and Mycosis Research and Prevention (No. ZZH2020004); The First Affiliated Hospital of Guangxi Medical University Provincial and Ministerial Key Laboratory

Cultivation Project: Guangxi Key Laboratory of Tropical Fungi and Mycosis Research (No. YYZS2020006); Guangxi Medical and Health Suitable Technology Development and Popularization Application Project (No. S2019090); the First Affiliated Hospital of Guangxi Medical University Clinical Research Climbing Program Youth Science and Technology Morning Star Program (No. 201903032); Advanced Innovation Teams and Xinghu Scholars Program of Guangxi Medical University.

CRedit authorship contribution statement

Wusheng Deng: conducted the experiments, analyzed the data, and wrote the manuscript. **Chuanlin Zhou:** conducted the experiments, analyzed the data, and wrote the manuscript. **Jiaoxia Qin:** conducted the experiments, analyzed the data, and wrote the manuscript. **Yun Jiang:** participated in the experiments and writing. **Xiujia Tang:** participated in the experiments and writing. **Jing Luo:** analyzed the data. **Jinliang Kong:** designed the study and participated in data, Formal analysis, and discussion. All authors read and approved the final version of the manuscript for submission. **Ke Wang:** designed the study and participated in data, Formal analysis, and discussion.

Declaration of competing interest

The authors declare that they have no known competing financial interests or personal relationships that could have appeared to influence the work reported in this paper.

Data availability

Data will be made available on request.

Appendix A. Supplementary data

Supplementary data to this article can be found online at <https://doi.org/10.1016/j.biofilm.2023.100174>.

References

- [1] Jamal M, Ahmad W, Andleeb S, et al. Bacterial biofilm and associated infections. *J Chin Med Assoc* 2018;81(1):7–11.

- [2] Wilkins M, Hall-Stoodley L, Allan RN, et al. New approaches to the treatment of biofilm-related infections. *J Infect* 2014;69(Suppl 1):S47–52.
- [3] Souza MC, dos Santos LS, Sousa LP, et al. Biofilm formation and fibrinogen and fibronectin binding activities by *Corynebacterium pseudodiphtheriticum* invasive strains. *Antonie Leeuwenhoek* 2015;107(6):1387–99.
- [4] Yin W, Wang Y, Liu L, et al. Biofilms: the microbial "protective clothing" in extreme environments. *Int J Mol Sci* 2019;20(14).
- [5] Rodríguez-Cerdeira C, Gregorio MC, Molares-Vila A, et al. Biofilms and vulvovaginal candidiasis. *Colloids Surf B Biointerfaces* 2019;174:110–25.
- [6] Suwal N, Subba RK, Paudyal P, et al. Antimicrobial and antibiofilm potential of *Curcuma longa* Linn. Rhizome extract against biofilm producing *Staphylococcus aureus* and *Pseudomonas aeruginosa* isolates. *Cellular and molecular biology (Noisy-le-Grand, France)* 2021;67(1):17–23.
- [7] Chen M, Yu Q, Sun H. Novel strategies for the prevention and treatment of biofilm related infections. *Int J Mol Sci* 2013;14(9):18488–501.
- [8] Sen CK, Roy S, Mathew-Steiner SS, et al. Biofilm management in wound care. *Plast Reconstr Surg* 2021;148(2):275e–88e.
- [9] Davies D. Understanding biofilm resistance to antibacterial agents. *Nat Rev Drug Discov* 2003;2(2):114–22.
- [10] Dostert M, Trimble MJ, Hancock REW. Antibiofilm peptides: overcoming biofilm-related treatment failure. *RSC Adv* 2021;11(5):2718–28.
- [11] Sharma K, Pagedar Singh A. Antibiofilm effect of DNase against single and mixed species biofilm. *Foods* 2018;7(3).
- [12] Xu Q, Sun F, Feng W, et al. [Effect of DNase I on biofilm formation of *Staphylococcus aureus*]. *Nan Fang Yi Ke Da Xue Xue Bao* 2015;35(9):1356–9.
- [13] Das T, Simone M, Ibugo AI, et al. Glutathione enhances antibiotic efficiency and effectiveness of DNase I in disrupting *Pseudomonas aeruginosa* biofilms while also inhibiting pyocyanin activity, thus facilitating restoration of cell enzymatic activity, confluence and viability. *Front Microbiol* 2017;8:2429.
- [14] Buzzo JR, Devaraj A, Gloag ES, et al. Z-form extracellular DNA is a structural component of the bacterial biofilm matrix. *Cell* 2021;184(23):5740–58. .e5717.
- [15] Slany M, Oppelt J, Cincarova L. Formation of *Staphylococcus aureus* biofilm in the presence of sublethal concentrations of disinfectants studied via a transcriptomic analysis using transcriptome sequencing (RNA-seq). *Appl Environ Microbiol* 2017; 83(24).
- [16] Zhao X, Liu Z, Liu Z, et al. Phenotype and RNA-seq-Based transcriptome profiling of *Staphylococcus aureus* biofilms in response to tea tree oil. *Microb Pathog* 2018; 123:304–13.
- [17] Deng W, Lei Y, Tang X, et al. DNase inhibits early biofilm formation in *Pseudomonas aeruginosa*- or *Staphylococcus aureus*-induced empyema models. *Front Cell Infect Microbiol* 2022;12:917038.
- [18] Schmittgen TD, Livak KJ. Analyzing real-time PCR data by the comparative C(T) method. *Nat Protoc* 2008;3(6):1101–8.
- [19] Al-Wrafy FA, Al-Gheethi AA, Ponnusamy SK, et al. Nanoparticles approach to eradicate bacterial biofilm-related infections: a critical review. *Chemosphere* 2022; 288(Pt 2):132603.
- [20] Qin N, Tan X, Jiao Y, et al. RNA-Seq-based transcriptome analysis of methicillin-resistant *Staphylococcus aureus* biofilm inhibition by ursolic acid and resveratrol. *Sci Rep* 2014;4:5467.
- [21] Wu Z, Zheng R, Zhang J, et al. Transcriptional profiling of *Pseudomonas aeruginosa* PAO1 in response to anti-biofilm and anti-infection agent exopolysaccharide EPS273. *J Appl Microbiol* 2021;130(1):265–77.
- [22] Liu CH, Di YP. Analysis of RNA sequencing data using CLC genomics workbench. *Methods Mol Biol* 2020;2102:61–113.
- [23] Ma L, Feng J, Zhang J, et al. *Campylobacter* biofilms. *Microbiol Res* 2022;264: 127149.
- [24] Tolker-Nielsen T. Biofilm development. *Microbiol Spectr* 2015;3(2). Mb-0001-2014.
- [25] Zhang L, Li J, Liang J, et al. The effect of Cyclic-di-GMP on biofilm formation by *Pseudomonas aeruginosa* in a novel empyema model. *Ann Transl Med* 2020;8(18): 1146.
- [26] Li J, Zhao X. Effects of quorum sensing on the biofilm formation and viable but non-culturable state. *Food Res Int* 2020;137:109742.
- [27] O'Toole GA, Kolter R. Flagellar and twitching motility are necessary for *Pseudomonas aeruginosa* biofilm development. *Mol Microbiol* 1998;30(2): 295–304.
- [28] Wassermann T, Meinike Jørgensen K, Ivanyshyn K, et al. The phenotypic evolution of *Pseudomonas aeruginosa* populations changes in the presence of subinhibitory concentrations of ciprofloxacin. *Microbiology (Read)* 2016;162(5):865–75.
- [29] Singh A, Rani K, Tandon V, et al. Ag NCs as a potent antibiofilm agent against pathogenic *Pseudomonas aeruginosa* and *Acinetobacter baumannii* and drug-resistant *Bacillus subtilis* by affecting chemotaxis and flagellar assembly pathway genes. *Biomater Sci* 2022;10(23):6778–90.
- [30] Valzano F, Boncompagni SR, Micieli M, et al. Activity of N-acetylcysteine alone and in combination with colistin against *Pseudomonas aeruginosa* biofilms and transcriptomic response to N-acetylcysteine exposure. *Microbiol Spectr* 2022;10 (4):e0100622.
- [31] Chen L, Zou Y, She P, et al. Composition, function, and regulation of T6SS in *Pseudomonas aeruginosa*. *Microbiol Res* 2015;172:19–25.
- [32] Corbitt J, Yeo JS, Davis CI, et al. Type VI secretion system dynamics reveals a novel secretion mechanism in *Pseudomonas aeruginosa*. *J Bacteriol* 2018;200(11).
- [33] Chen L, Zou Y, Kronfl AA, et al. Type VI secretion system of *Pseudomonas aeruginosa* is associated with biofilm formation but not environmental adaptation. *MicrobiologyOpen* 2020;9(3):e991.
- [34] Lee KJ, Kim JA, Hwang W, et al. Role of capsular polysaccharide (CPS) in biofilm formation and regulation of CPS production by quorum-sensing in *Vibrio vulnificus*. *Mol Microbiol* 2013;90(4):841–57.
- [35] Petrucci B, Briggs RE, Tatum FM, et al. Capsular polysaccharide interferes with Biofilm Formation by *pasteurella multocida* serogroup A. *mBio* 2017;8(6).
- [36] Salimena AP, Lange CC, Camussone C, et al. Genotypic and phenotypic detection of capsular polysaccharide and biofilm formation in *Staphylococcus aureus* isolated from bovine milk collected from Brazilian dairy farms. *Vet Res Commun* 2016;40 (3–4):97–106.
- [37] George SE, Nguyen T, Geiger T, et al. Phenotypic heterogeneity and temporal expression of the capsular polysaccharide in *Staphylococcus aureus*. *Mol Microbiol* 2015;98(6):1073–88.
- [38] Wessels MR. Capsular polysaccharide of group A *Streptococcus*. *Microbiol Spectr* 2019;7(1).
- [39] Xia FD, Mallet A, Caliot E, et al. Capsular polysaccharide of Group B *Streptococcus* mediates biofilm formation in the presence of human plasma. *Microb Infect* 2015; 17(1):71–6.
- [40] DeFrancesco AS, Masloboeva N, Syed AK, et al. Genome-wide screen for genes involved in eDNA release during biofilm formation by *Staphylococcus aureus*. *Proc Natl Acad Sci U S A* 2017;114(29):E5969–e5978.